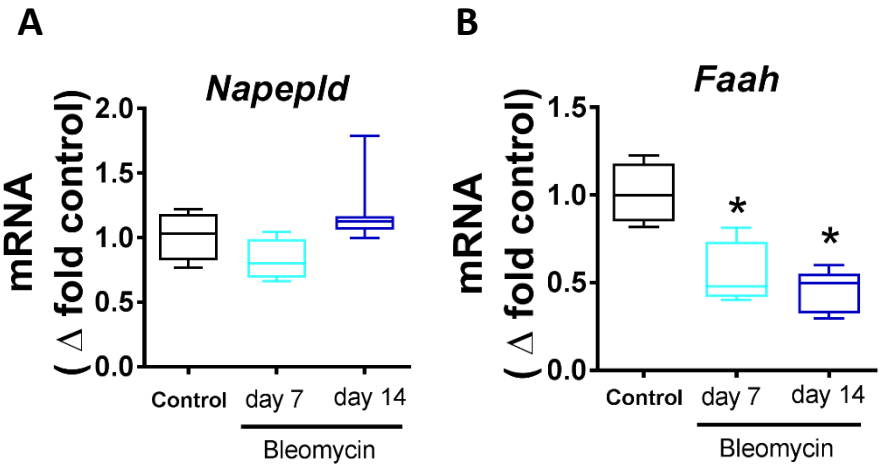

Supplemental Figure 1. Expression of AEA biosynthetic and AEA degrading enzymes in lung in BL-PF. Gene expression of *N*-acyl-specific phosphatidylethanolamine phospholipase D (*Napepld*) (**A**) and fatty acid amide hydrolase (*Faah*) (**B**) in mouse lung before and 7 or 14 days after bleomycin treatment. Data represent box and whisker plots, the horizontal line in the box is the median and 25th to 75th percentiles, and whiskers represent minimum and maximum values from 4 mice per group for control and day 7, and 5 mice per group for day 14. Data were analyzed by one-way ANOVA followed by Dunnett's multiple comparisons test. *($P<0.05$) indicates significant difference relative to control group.

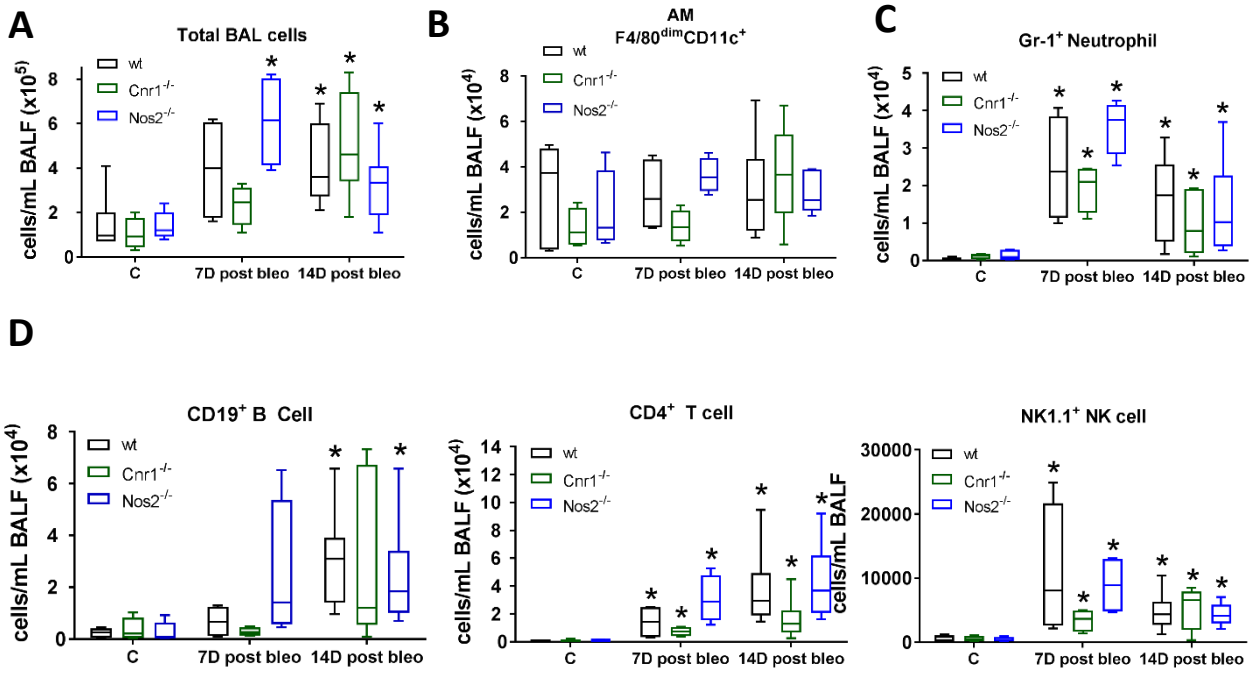

Supplemental Figure 2 : Effect of *Cnr1* and *Nos2* gene deletion on BAL cell populations. Flow-cytometry analysis of BALF-cells from wt, *Cnr1*$^{-/-}$ and *Nos2*$^{-/-}$ mice with either control (C), post-bleomycin day 7 group (7D post bleo) or post-bleomycin day 14 group (14D post bleo). Total cell number (**A**), alveolar macrophages (AM) (**B**), neutrophils (**C**), and lymphocytes (**D**) present in the BALF, n=6 (wt), 4 (*Cnr1*$^{-/-}$) 5 (*Nos2*$^{-/-}$). Data represent box and whisker plots, the horizontal line in the box is the median and 25th to 75th percentiles, and whiskers represent minimum and maximum values . * (P<0.05) indicates significant difference from control group (t-test). $^{\#}$ (P<0.05) indicates significant difference from the corresponding strain in the post-bleomycin group (two-way ANOVA followed by multiple comparisons test).

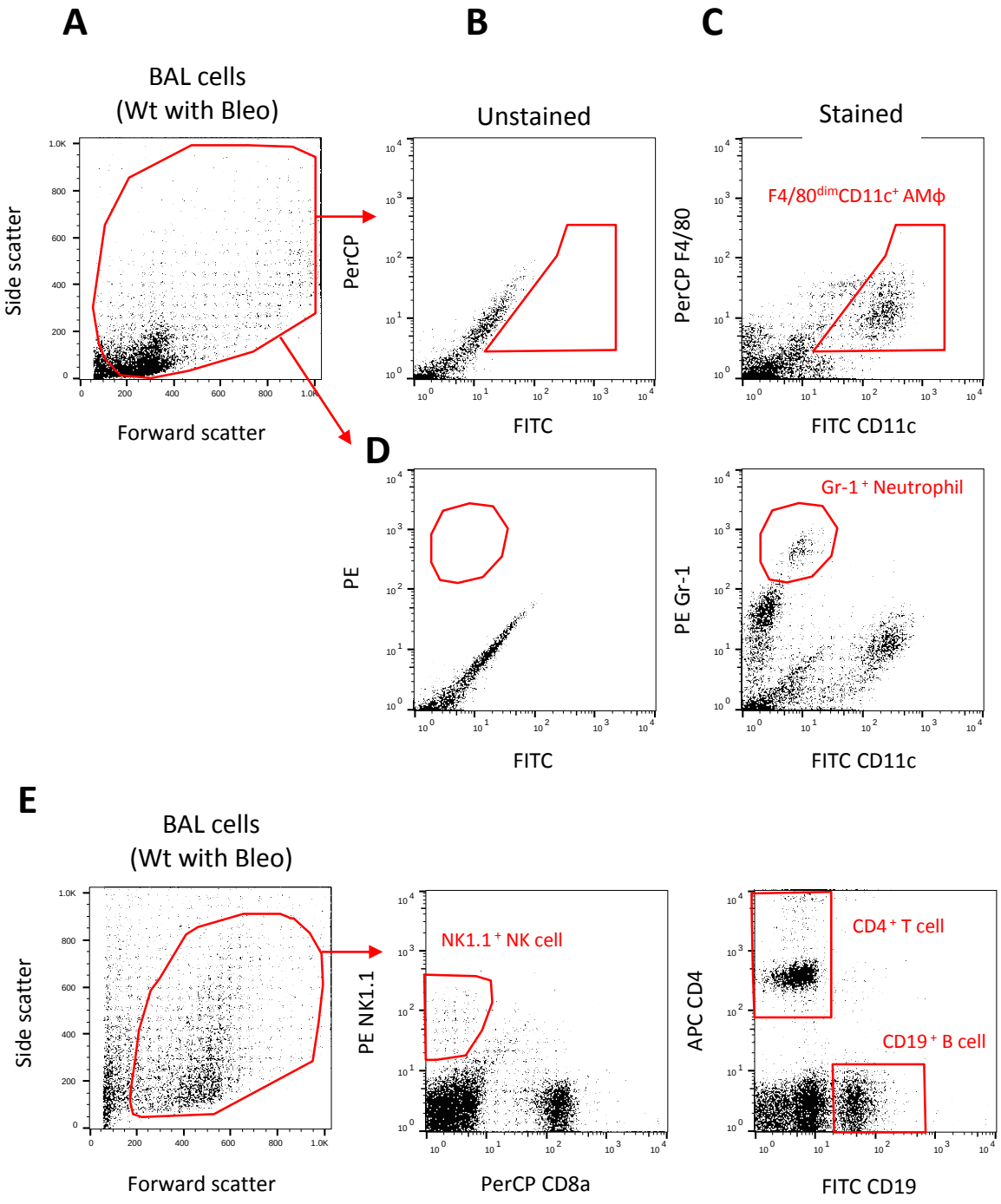

Supplemental Figure 3: Gating strategy for alveolar macrophages, neutrophils and lymphocytes in Flow-Cytometry. Alveolar Macrophages (AMΦs) were gated using FSC/SSC channel to exclude cell debris (**A**). Autofluorescence of BAL cells was assessed using unstained cells (**B**), and AMΦs were then defined as autofluorescence positive, F4/80 dim, CD11c^{+} population (Auto^{+}F4/80^{dim}CD11c^{+}) (**C**), Neutrophils are gated as shown (**D**), Lymphocytes were gated by cell size and defined by lymphocyte-specific markers (**E**).

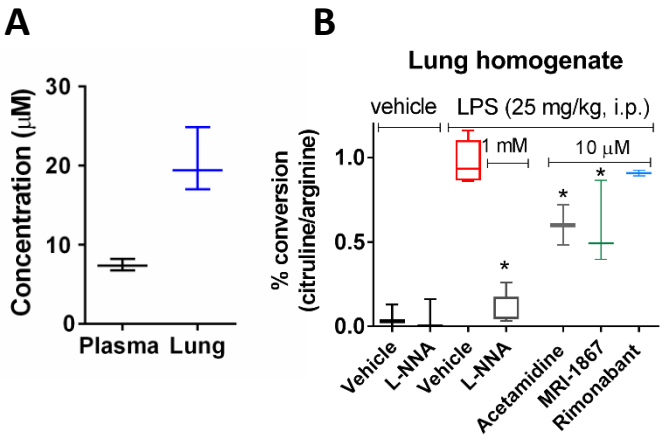

Supplemental Figure 4: Target engagement by MRI-1867 in lung. **A:** Plasma and lung levels of total (bound + free) MRI-1867 1h after acute oral dosing at 10 mg/kg. **B:** Effect of MRI-1867 and rimonabant on iNOS activity in lung homogenates from mice pre-treated with LPS 6h before tissue harvesting. L-NNA (Nω–nitro-L-arginine, 100 μM) was used as positive control in iNOS activity assay. Data represent box and whisker plots, the horizontal line in the box is the median and 25th to 75th percentiles, and whiskers represent minimum and maximum values, n=3 mice per group; *($P<0.05$) indicates significant inhibition of LPS-induced iNOS activity.

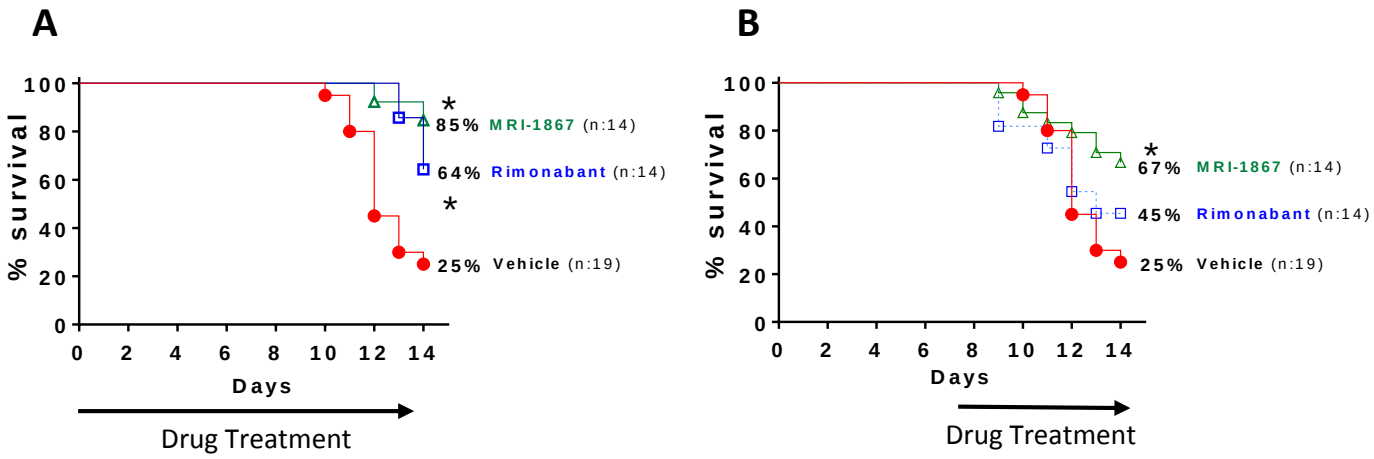

Supplemental Figure 5: MRI-1867 improves survival at a submaximal oral dose. Survival curve for fibrosis prevention (**A**) and arrest of progression (**B**) treatment paradigms in bleomycin-instilled mice following chronic treatment with vehicle, rimonabant, or MRI-1867 (3 mg/kg, PO). The length of vehicle treatment (starting at day 0 or 7) did not significantly affect survival, therefore these data were merged and used as control for both treatment paradigms, as shown in **A** and **B**. * (P<0.05) indicates significant difference from bleomycin-challenged, vehicle-treated group.